*Solar-Terrestrial Physics. 2024. Vol. 10. Iss. 1. P. 54–62. DOI: 10.12737/stp-101202408. © 2024 A.G. Sorokin, V.A. Dobrynin. Published by INFRA-M Academic Publishing House*

UDC 534-6, 550.34.06, 550.34.09
DOI: 10.12737/stp-101202408

Received June 26, 2023
Accepted December 13, 2023

# REGISTRATION OF THE ATMOSPHERIC EFFECT OF THE HUNGA TONGA VOLCANO ERUPTION

**A.G. Sorokin**
*Institute of Solar-Terrestrial Physics SB RAS, Irkutsk, Russia, sor@iszf.irk.ru*

**V.A. Dobrynin**
*Institute of Solar-Terrestrial Physics SB RAS, Irkutsk, Russia, dobrynin@iszf.irk.ru*

**Abstract.** The paper presents the results of recording of acoustic waves, caused by the Hunga Tonga volcano eruption in the South Pacific Ocean on January 15, 2022, in Eastern Siberia at a distance of about 11230 km from the eruption. The received acoustic signal is interpreted as a set of atmospheric waves in a wide range of oscillations. The structure of the signal is similar to signals from the previously known powerful sources: the thermonuclear explosion on Novaya Zemlya in 1961 and the explosion of the Tunguska meteorite in 1908. The acoustic signal was preceded by three trains of low-frequency damped oscillations. We assume that these three trains of oscillations are associated with three important stages in the Hunga Tonga volcano eruption: 1) destruction of Tonga island and formation of an underwater caldera; 2) release of hot magma from the caldera to the ocean surface and release of a large volume of superheated steam into the atmosphere 3) formation of a layered structure from a mixture of superheated steam, ash, and tephra on the ocean surface and formation of an eruptive convective column. Successive phases of the eruption might have contributed to the excitation of acoustic vibrations in a wide range of periods including Lamb waves, internal gravity waves (IGW), and infrasound. We compare the structure of the acoustic signal received in Siberia at a distance of more than 11000 km from the volcano and that of the acoustic signal recorded in Alaska at a distance of more than 9300 km. Using the solution of the linearized Korteweg — de Vries equation, we estimate the energy released during the volcanic eruption.

**Keywords:** atmosphere, acoustic wave, Lamb wave, infrasound, volcanic eruption, Tunguska meteorite, homogeneous atmosphere, eruption energy.

## INTRODUCTION

On January 15, 2022 at 04:14:45 UTC, a great eruption of the Hunga Tonga-Hunga Ha'apai volcano occurred in the South Pacific Ocean. According to local authorities, the area of the eruption was ~5 km$^2$, the depth of the formed underwater caldera was ~200 m. As recorded by the Geophysical Survey of the Russian Academy of Sciences, the geographic coordinates of the Hunga Tonga volcano eruption are 20.546 S and 175.39 E, the magnitude of its associated earthquake $M$=5.8.

The eruption was accompanied by a number of geophysical phenomena — tsunamis, seismic processes, and strong disturbances at different heights in the atmosphere and ionosphere [Adam, 2022; Duncombe, 2022; Vergoz et al., 2022; Garova, Ferapontov, 2022].

Atmospheric pressure waves generated by the Hunga Tonga eruption were recorded in various parts of the globe at stations of the International Monitoring System (IMS). In Russia, the pressure waves were detected in the Far East [Dolgikh et al., 2022], in Siberia [Dobrynin, Sorokin, 2023], and in the central part of Russia (in the Moscow Region) [Kulichkov et al., 2022; Rybnov et al., 2023]. The acoustic signals that have circuited the globe at least twice represent, according to many authors, a superposition of atmospheric waves of several types such as infrasonic vibrations, gravity and Lamb waves. It is generally believed that Lamb waves, which occur during volcanic eruptions and nuclear explosions, are the main energy-carrying mode when passing along Earth's surface [Kulichkov, 1987; Gossard, Hook, 1978]. These waves are a two-dimensional atmospheric analogue of Lamb waves propagating in the real atmosphere at the speed of sound and with periods exceeding the Brunt — Väisälä periods [Pierce, Pousey, 1971; Gossard, Hook, 1978]. The geophysical effects of the Hunga Tonga-Hunga Ha'apai volcano eruption on January 15, 2022 at a great distance from the source are discussed by Adushkin et al. [2022]; the authors describe electric field variations associated with the passage of an acoustic wave from the Hunga Tonga volcano.

Attempts have been made to estimate the energy released during the Hunga Tonga volcano eruption [Vergoz et al., 2022; Rybnov et al., 2023; Kulichkov et al., 2022]. For example, Kulichkov et al. [2022] have used an assumption that the main energy-carrying mode from a volcanic eruption is a low-frequency Lamb wave. By relying on the solution of the linearized Korteweg–de Vries equation derived by Pierce, Pousey [1971], the authors presented an expression for estimating the released energy, in which the key parameters are the amplitude and the corresponding period of the first oscillation for the Lamb wave [Kulichkov et al., 2022].

Propagation of the acoustic wave from the Hunga Tonga volcano eruption was global, and its passage was detected at great distances from the source [Matoza et al., 2022]. On the official Twitter account of the National Weather Service (NWS) Alaska Region, a report was posted on January 15, 2022 about detection of an acoustic signal from the Hunga Tonga volcano eruption in Alaska [https://twitter.com/NWSAlaska/status/1482431322740060162?cxt=HHwWhMCrveHb05IpAAAA], which con-

tained information about the moment of arrival of the acoustic signal, its spectral composition, amplitude, duration, etc. (Figure 5).

In this paper, we present data on recording of an acoustic signal from the Hunga Tonga volcano eruption in Eastern Siberia and give our own original interpretation of the successive phases of the volcanic eruption and the acoustic signal structure, i.e. Lamb waves preceding the recorded signal (Figures 1, 4).

## PURPOSE AND OBJECTIVES OF THE STUDY

Our main purpose is to study structural features of the infrasonic signal recorded from the remote strong Hunga Tonga volcano eruption on January 15, 2022. To achieve this purpose, we had to solve the following problems:

- to prepare recording data at the ISTP SB RAS infrasound station;
- to analyze the strongest eruptions of the XIX–XXI centuries and to determine where the Hunga Tonga volcano eruption is in this series;
- to compare the two acoustic signals from the Hong Tonga volcano eruption recorded in Eastern Siberia and Alaska, which propagated in different azimuthal directions along paths of different lengths;
- to identify possible causes for the differences between the acoustic signals, including meteorological conditions along propagation paths;
- using the method presented in [Pierce, Pousey, 1971], to estimate the energy of the Hunga Tonga volcano eruption.

## HISTORICAL BACKGROUND

The International Monitoring System (IMS) is employed to monitor not only nuclear explosions, but also high-power natural events associated with major volcanic eruptions, explosions of large meteorites, etc., which are of serious hazard to the population. Creation and development of IMS [Brachett et al., 2010] boosted the research in atmospheric acoustics.

On March 27, 1954 at the Bikini Atoll in the Marshall Islands, the United States tested the world's first thermonuclear bomb, acoustic waves from which reached Japan and were recorded at a distance of ~3900 km [Yamomoto, 1954]. Acoustic signals from the Soviet thermonuclear bomb with a capacity of 57 Mt tested on Novaya Zemlya in October 1961 had a structure similar to signals from volcanic eruptions [Donn, Ewing, 1962], and due to the enormous yield of the explosion passed around the globe several times; the signals were recorded in the north of Scotland (Aberdeen) [Gossard, Hook, 1978; Donn, Ewing, 1962; Carpenter et al., 1961]. The acoustic signals were analyzed and compared with the previously observed atmospheric waves from the Krakatoa volcano eruption in 1883 and with the atmospheric effect of the Tunguska meteorite in 1908. Comparative analysis of natural signals and theoretical barograms for a multilayer medium made it possible to explain the structure of the received acoustic signal [Harkrider, 1964]. In the 1970s, the theory of excitation of the fundamental mode of Earth's atmosphere oscillations was developed [Pierce, Pousey, 1971]. The first attempt to apply the fundamental mode theory in practice to atmospheric characteristics was made in [Garrett, 1969]. The use of the fundamental mode theory in Russia is analyzed in [Kulichkov, 1987].

## RETROSPECTIVE ANALYSIS OF VOLCANIC ACTIVITY ACCORDING TO THE VEI INDEX

The brief analysis of volcanic activity from 1815 to the present time (see Table) suggests that powerful volcanic eruptions are quite rare and occur about once every 100 years.

Table shows that according to the volcanic explosivity index (*VEI*=7) the Tambora volcano eruption in 1815 was in the lead during the pre-instrumental era. The closest according to *VE*I (*VEI*=6) to the Hunga Tonga volcano eruption are the eruptions of Krakatoa in 1883 and Pinatubo in 1991.

## BASIC FACTS ABOUT THE HUNGA TONGA VOLCANO ERUPTION

In the southeastern Pacific Ocean between Australia and New Zealand, a strong eruption near Hunga Tonga-Hunga Ha'apai Island ~2 km long occurred on January 15, 2022. The first eruption on January 14 released an ash plume ~5 km wide into the atmosphere, which rose to a height of more than 20 km. The next day, at about 17:15 LT (04:14:45 UT), a larger eruption began. Ash mass emissions reached heights of more than 30 km. Strong explosions were heard at a distance of 65 km from the epicenter. The explosions were also heard throughout New Zealand, Canada, and Alaska. NASA's Aqua satellite detected shock waves propagating in the atmosphere over the Pacific Ocean almost simultaneously with the eruption [Duncombe, 2022].

Analysis of volcanic activity in the XIX–XXI centuries.

| Name | *VEI* | Type of eruption | Eruption height, km | Eruption volume, $km^3$ | Temperature drop, °C | Detection range |
|---|---|---|---|---|---|---|
| Tambora, 1815 | 6–7 | Plinian | 43 | 100 $km^3$ | –1 to –5 | no data available |
| Krakatoa, 1883 | 6 | Plinian | 36 (up to 70) | 10 $km^3$ | –0.3 | Africa, English Channel |
| St. Helens, 1980 | 4–5 | no data available | 19 | 1 $km^3$ | – | USA |
| Pinatubo, 1991 | 5–6 | Plinian | 34 | 10 $km^3$ | –0.5 | Southeast Asia |
| Hunga Tonga, 2022 | 5–6 | Plinian | 30–37 | $0.4 \cdot 10^6$ t $(SO)_2$ | local | round-the-world |

## STRUCTURE OF ACOUSTIC OSCILLATIONS IN THE ATMOSPHERE ACCORDING TO ISTP SB RAS DATA AND THEIR CONNECTION WITH SEISMIC EVENTS

Analysis of the sequence of acoustic signal trains is based on data acquired at the infrasound station (51°48′55.49″ N, 103°04′14″ E) of the ISTP SB RAS Geophysical Observatory, located in the south of Eastern Siberia in the Tunka District of the Republic of Buryatia. This station is a group of three microbarometers located at vertices of a right triangle with 500 m legs. Three independent microbarometers forming an interferometer record successive arrivals of an acoustic wave. The main parameters of the infrasound station are described in [Sorokin, 2013]. The acoustic signal received by the infrasound station (see Figure 1) can be interpreted as follows.

1. Arrival of the very first and strongest low-frequency signal (group 1) at 14:26:42 UT corresponds to the initial phase of the major explosion, the destruction of the island, and the formation of an underwater caldera with red-hot magma.

2. The second part of the low-frequency acoustic signal (group 2) is likely to correspond to the eruption phase when hot magma interacts with ocean water and an above-water pulsating cloud layer consisting of superheated steam is formed.

3. We suspect that the arrival of group 3 of the low-frequency acoustic signal is related to the emission of acoustic waves by a ~30 km high-altitude convective column formed from a mixture of superheated steam and volcanic ejecta. The mechanism of such emission was described by Gostintsev et al. [1985], using a big fire as an example.

Arrival of group 3 in the signal structure is followed by oscillations in the infrasound range, which are related to the volcanic eruption and last for about 5 hrs.

A similar sequence of explosive events of the Hunga Tonga volcano eruption is presented in [Astafyeva et al., 2022] without indicate the conformance to certain events. Studying volcanic ionospheric disturbances of the total electron content (TEC) shows that five explosive volcanic events occurred from 4 to 5 UT. It is interesting that these TEC variations are not similar in shape to the quasi-periodic signal observed in previous studies. These volcanic ionospheric disturbances are complex signals with the apparent appearance of N-waves with a sharp increase in TEC, which, according to Astafyeva et al. [2022], indicates the source of a shock acoustic wave.

Such an event scenario fits well into the picture described in [Wright et al., 2022] as a series of five atmospheric pressure pulses recorded during the same time period near (64 km) the Hunga Tonga volcano eruption.

Arrival of group 1 consisting of the most intense oscillations is the main energy-carrying mode of the acoustic signal — the Lamb wave. It is almost the first to be excited during a volcanic eruption; it propagates along Earth's surface at a speed close to the speed of sound [Kulichkov, 1987; Kulichkov et al., 2022]. Accordingly, this low-frequency mode is manifested in recordings of the acoustic station recorder at the very beginning. What are these oscillations? Let us turn to the classical work [Maeda, Young, 1966], where the dispersion equation for atmospheric waves is derived from three fundamental equations: motion equation, the continuity equation, and equation of thermodynamics. Their combination yields an equation for the vertical variation of wave velocity. Studying the determinant of this equation leads to cases where roots of the equation are real or imaginary, i.e. from its analysis we have three branches of oscillations:

1) $\omega > \omega_A > \omega_B$ — such frequencies correspond to a purely acoustical branch of oscillations;

2) $\omega < \omega_A < \omega_B$ — such frequencies correspond to the gravity branch of oscillations;

3) $\omega_A > \omega > \omega_B$ — at these frequencies there is a branch of surface oscillations (Lamb waves).

Here, $\omega_A$ is the atmospheric resonance frequency, $\omega_B$ is the Brunt — Väisälä frequency.

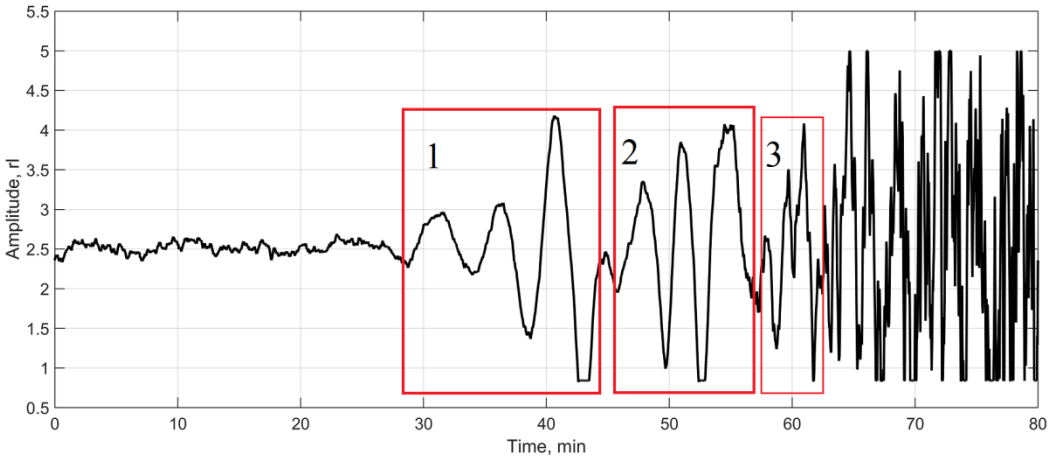


*Figure 1*. Low-frequency acoustic signal received at the ISTP SB RAS infrasound station on January 15, 2022 (1, 2, 3 — wave trains). It began at 14:26:42 UT. The total duration of the signal is more than 5 hrs

Indeed, we are observing a wave with an oscillation period of 5.4 min. This corresponds to the third branch of oscillations, and these are not classical acoustic waves or internal gravity waves (IGWs). Since the mean velocity of wave propagation along the path is estimated from observations and is 305 m/s, it is these oscillations that represent a fast surface Lamb wave.

A volcanic eruption is a nonstationary process and is accompanied by alternating volcanic explosions and ejecta, which, in turn, are followed by intense sonic noise, including infrasonic signals having a sonic propagation velocity. That is why the infrasonic noise from a volcanic eruption is the second to arrive at the acoustic station.

If we follow these arguments, we will deduce that a group of signals from an eruption associated with IGWs having a relatively low velocity should appear in the final part of the signal wave train. This is, however, not observed. Satellite data obtained in [Liu et al., 2022] indicates that the spatial zone of observation of IGWs from the eruption is limited, and IGWs are not recorded at a great distance from the eruption, probably due to dissipation.

Our calculations of the emission power spectra of acoustic signals (train 1 – train 3) have shown three main harmonics (Figure 2). For the time interval of 240000 readings ($t$~80 min), the Hemming function (Hemming application (92160, 46080, 46080, 50, 0)) was used for the calculations in Mathlab. There are several characteristic wave periods in the head part of the signal: $T_1$~322.6 s; $T_2$~192.3 s; $T_3$~106.4 (5.4 min, 3.2 min, 1.8 min respectively).

Research on infrasonic waves has a long history. In [Gordeev et al., 2013; Fee, Matoza, 2013], infrasonic waves from volcanic eruptions in Kamchatka and Alaska are examined. The works [Dessler, 1973; Yerushchenkov et al., 1976; Pasko, 2009; Sorokin, Dobrynin, 2022] deal with infrasound from lightning discharges. Martinez-Bedenko et al. [2023] provides information on unusually high lightning activity during the Hunga Tonga volcano eruption. In fact, the lightning activity zone of the eruption is fairly broad [https://www.reuters.com/graphics/TONGA-VOLCANO/LIGHTNING/zgpomjdbypd/]. The strong lightning discharges that excite infrasonic waves with characteristic frequencies 0.5–5 Hz are, however, significantly bounded by the atmospheric region, where intense volcanic ejecta and convective flows of volcanic gases in the form of eruptive columns ~30–40 km and 20–25 km long are observed. When propagating over long distances in the atmosphere, infrasonic oscillations in the high-frequency region (0.5–5 Hz) are subject to strong molecular absorption; therefore, there is no noticeable contribution of infrasonic signals from lightning discharges, excited at the epicenter of the eruption, to the signal recorded at a large distance from the eruption.

The eruption of the underwater Hunga Tonga volcano on January 15, 2022 caused a number of geophysical responses including a strong seismic signal. According to [Thurin et al., 2022], the magnitude of the earthquake accompanying the eruption Mw~6.3. The USA Seismic Station (Fiji Island area) at a distance of ~700 km southwest of the Hunga Tonga volcano eruption recorded several successive seismic events during the initial phase of the eruption (Figure 3).

Comparison of acoustic signals recorded at the ISTP SB RAS infrasound station (see Figure 1) with variations in seismic activity during the initial phase of the eruption on January 15, 2022 detected at the seismic station in the Fiji Island area (see Figure 3), shows that in both cases there is a similar sequence of three strong explosions associated with the eruption.

First red line S1 in Figure 3 indicates surface seismic waves traveling at a Rayleigh wave speed (~3600 m/s), delayed by 32.5 s relative to the time of the eruption according to the USGS (US Geological Survey) catalog. The second Rayleigh wave train (red dashed line S2) arrives 200 s later. The total duration of such seismic signals for this case is ~400 s. Thurin et al. [2022] report that there might have been additional events; the third gray strip highlights signals from a probable third seismic event. The blue dashed line shows propagation of an acoustic wave of atmospheric pressure at a velocity of 340 m/s.

## COMPARING ACOUSTIC SIGNALS FROM THE JANUARY 15, 2022 HUNGA TONGA VOLCANO ERUPTION, RECEIVED IN SIBERIA AND ALASKA

The experience of observing propagation of acoustic waves from previous major eruptions (Krakatoa 1883; Pinatubo 1991) bears witness to the global nature of the events. Comparison of observations in Eastern Siberia (ISTP SB RAS, Irkutsk, Russia) at a distance of 11230 km (Figure 4) and in Alaska (Alaska Volcano Observatory, University of Alaska Fairbanks, Fairbanks, USA) at a distance of 9360 km (Figure 5) from the epicenter of the eruption clearly proves global propagation of acoustic waves in the atmosphere from the Hunga Tonga volcano eruption. The nature of the acoustic signals is seen to be generally similar, except for some details that can be attributed to the different length of propagation paths, different meteorological conditions along the paths, and differences in recording equipment. The following facts are confirmed: a) the global nature of propagation of such waves; b) the high intensity of acoustic wave radiation (as in the case of the Krakatoa eruption in 1883).

The signal propagation time to Eastern Siberia was about 10 hrs 13 min; to Alaska, 8 hrs 15 min. The mean propagation velocities of the acoustic signal turned out to be different, 305 and 315 m/s respectively, which is likely to be explained by different lengths of the signal propagation paths and meteorological conditions along the paths.

Figures 6 and 7 display height cross-sections of the wind field in the atmosphere, plotted from ERA5 reanalysis weather data (along the Y-axis are heights to 50 km; along the X-axis, the distance from the Hunga Tonga volcano (right) to the receiving station (left). Along the Tonga — Irkutsk path (~11230 km), the predominant wind

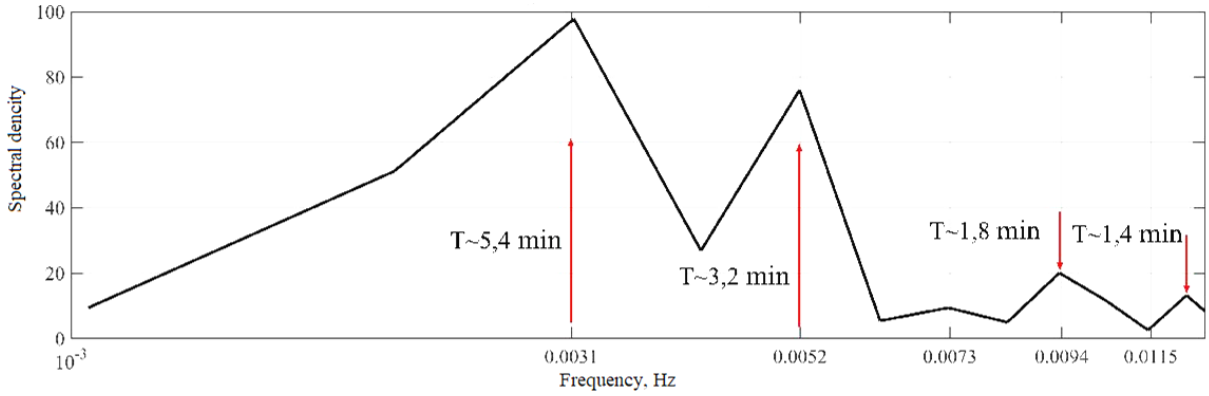


*Figure 2*. Spectrum of low-frequency oscillations of the acoustic signal recorded at the ISTP SB RAS station on January 15, 2022: $T_1$~322.6 s = ~5.4 min; $T_2$=192.3 s ~3.2 min; $T_3$=106.4 s ~1.8 min

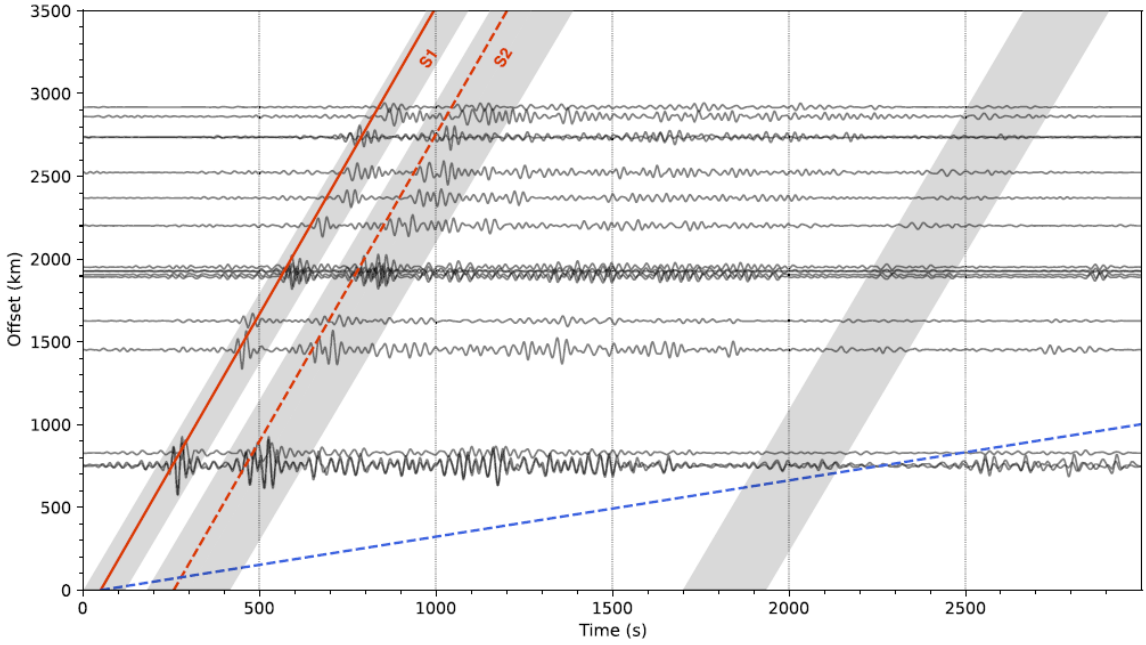


*Figure 3*. Seismograms of the vertical component recorded on Fiji Island. The data is filtered in the range of periods 25–70 s. The blue dashed line indicates an acoustic wave of atmospheric pressure traveling at a speed of 340 m/s [Thurin et al., 2022]

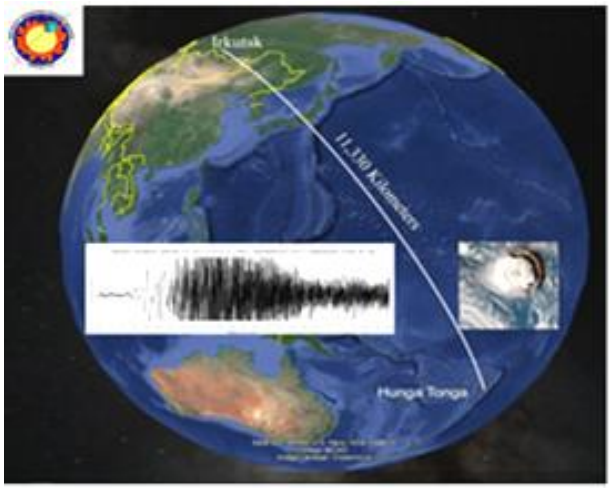


*Figure 4*. Acoustic waves from the January 15, 2022 Hunga Tonga volcano eruption recorded in Irkutsk (ISTP SB RAS, Eastern Siberia, Russia)

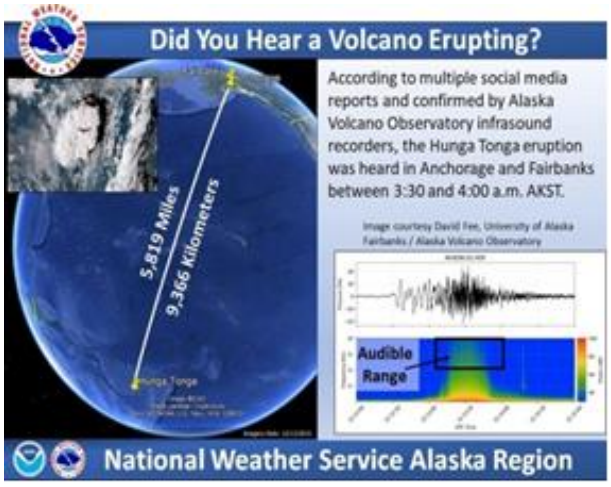


*Figure 5*. Acoustic waves from the January 15, 2022 Hunga Tonga volcano eruption recorded in Anchorage and Fairbanks (NWS Alaska Region Report dated January 15, 2022 [https://twitter.com/NWSAlas ka/status/1482431322740060162?cxt=HHwWhMCrveHb05IpAAAA])

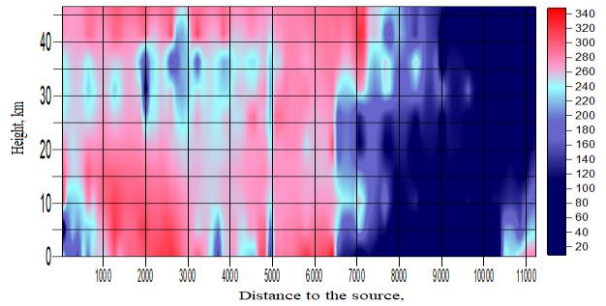


*Figure 6.* Height wind directions along the Tonga—Irkutsk path (Tonga is on the right)

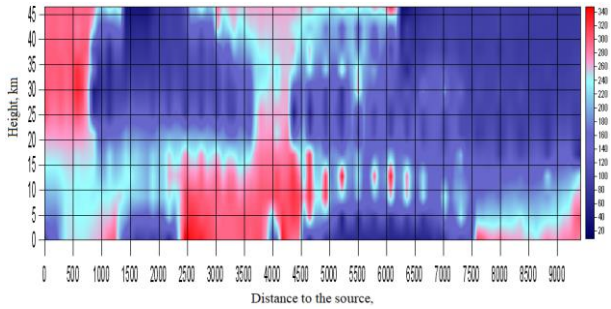


*Figure 7.* Height wind directions along the Tonga—Alaska path (Tonga is on the right)

wind direction is seen to coincide with the direction of propagation of the acoustic signal, whereas along the Tonga — Alaska path (9360 km) the winds directed almost across the propagation path prevail. Hence, the differences in the average propagation velocity and the shape of acoustic signals may be related to the different structure of the wind field along the paths.

## ESTIMATED ENERGY OF THE HUNGA TONGA VOLCANO ERUPTION

Considering the possibility of estimating the energy of a volcanic eruption as equivalent to a surface explosion, Pierce and Pousey [1971] derived a solution of the linearized Korteweg — de Vries equation (KdV) for the Lamb mode in the following form:

$$\psi(t, s, \theta) = \frac{T_\gamma}{\tau_D}\pi^{-1/2}\int_0^\infty Ai\left(\frac{\tau_a - t}{\tau_D} + \mu\frac{T_\gamma}{\tau_D}\right)M(\mu)\,d\mu. \quad (1)$$

Here $\psi(t, s, \theta)$ is the wave function; $t$ is the current time; $s$ and $\theta$ are curved cylindrical coordinates with the origin ($s$=0) near the source; $\theta$ is the azimuth of the ray exit angle; $T_\gamma$ is the characteristic explosion time; $\tau_D$ is the characteristic time scale of dispersion for the Lamb wave [Pierce, Pousey, 1971]. Allowing for the sphericity of Earth's surface, the time of passage of the Lamb mode $\tau_a$ along the curved ray path with given $\theta$ from $s$=0 to a point at a distance $s$ from the source is given by the formula $\tau_a = \int_0^s ds / c_e$, where $c_e$ is the average Lamb mode velocity that takes into account: a) the height-averaged component of the wind speed along the ray path (it is believed that the wind speed is lower than the speed of sound); b) height-averaged deviations of the speed of sound and wind speed from their values in an isothermal atmosphere (constant speed of sound) at a constant wind speed. The function $M(\mu)$ describes the waveform of the signal generated by the source at a distance close to it. The so-called Glasstone pulse is often utilized as a model of the signal generated by an explosion: $M(\mu)\equiv p(t)=\Delta p(t-t/T_\gamma)\exp(t—t/T_\gamma)$, where $t$ is the current time, $\Delta p$ and $T_\gamma$ are the amplitude and the duration of the positive compression phase of this pulse respectively, and $\mu=t/T_\gamma$. The waveform of signal $\psi(1)$ is determined by the Airy function Ai($x$) and for $T_\gamma/\tau_D$~0.5 is shown in Figure 8 as a function of dimensionless time $(\tau_a-t)/\tau_D$.

For these conditions, we have made an attempt to estimate the energy of the Hunga-Tonga volcano eruption. The estimation technique is described in [Kulichkov et al., 2022] and is as follows. Using the solution of the linearized KdV equation [Pierce, Pousey, 1971], we calculate a model of an acoustic signal in the atmosphere with dispersion properties close to the real acoustic signal. By selecting the parameters, a satisfactory similarity is achieved, and the characteristic time scale of the dispersion is estimated at a distance close to the source.

With a sufficiently short explosion time, $T_\gamma\,(\mu \ll 1)$, which occurs in the case under study, at distances of several thousand kilometers from the source, the waveform of the signal stabilizes, and the signal takes the form of (1) [Pierce, Pousey, 1971; Kulichkov, 1987].

In our case, an adequate similarity of the model (for the Glasstone pulse) and the real signal is achieved with the following parameters: during the initial period $T_\gamma$=1 of the acoustic signal in the source (the duration of the positive phase of the Glasstone pulse) when propagating in an atmospheric medium with a characteristic time scale of dispersion, the signal period blurs and doubles already at $(\tau_a-t)/\tau_D$=40 [Pierce, Pousey, 1971; Kulichkov, 1987].

Thus, we believe that the artificial signal obtained by solving the KdV equation is close to the real acoustic signal for which we can use the ratio to estimate energy [Pierce, Pousey, 1971] $E = 13P\left(r_E \sin\left(r / r_E\right)\right)^{1/2} \times$ $\times H_s\left(cT_{1,2}\right)^{3/2}$.

The explosion energy of the volcano $E$ is estimated from the following parameters of the observed acoustic signal and atmospheric parameters: the amplitude of the acoustic signal $P$=184 Pa, the Earth radius $r_E$=6400 km,

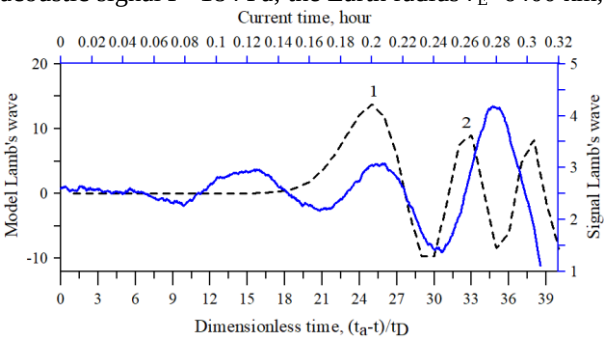


*Figure 8.* Atmospheric analogue of the two-dimensional Lamb wave recorded at the ISTP SB RAS infrasound station (solid blue curve), and the Lamb wave model obtained from the solution of the linearized Korteweg — de Vries equation (dashed curve)

the source — receiver distance $r$=11230 km, the height of the homogeneous atmosphere $H_s$=8 km, the period of the first oscillation train $T_{1,2}$=330 s. For these parameters, $E = 1.631 \cdot 10^{18}$ J or $E = 0.398 \cdot 10^{6}$ t in TNT equivalent.

Alternative approaches for estimating the eruption energy are based on statistical analysis of the energy release for a large number of explosions of various types and comparison with the energy characteristics of earthquakes and other eruptive phenomena. Such a technique involves plotting an empirical dependence of the period $T$ of pressure waves excited in the atmosphere on the explosive yield $W$.

For example, Edwards et al. [2006] have developed and refined the empirical relationships linking the periods of infrasonic waves during meteoroid explosions to the energy of their destruction. The aim of their work [Edwards et al., 2006] was to obtain empirical relationships from a large amount of data on explosions of various types, in particular to investigate the statistical properties of infrasonic signals in terms of atmospheric winds. The empirical relationships derived were used to estimate the energy of meteoroid explosions of previously recorded infrasound events.

The most general empirical relationship was developed for the American Air Force Technical Applications Center (AFTAC) back in 1997 [ReVelle, 1997]:

$$\log(W/2) = 3.34 \log T - 2.58 \quad \text{for } W/2 \le 100 \text{ kt}; \qquad (1a)$$

$$\log(W/2) = 4.14 \log T - 3.61 \quad \text{for } W/2 \ge 40 \text{ kt}. \qquad (1b)$$

Here $W$ is the energy of the meteoroid in kilotons of TNT equivalent; $T$ is the period of an infrasonic wave of maximum amplitude in seconds for two energy ranges [Sorokin, 2013]. Ratio (1a) for the upper energy range yields $W/2 \approx 0.639$ Mt; ratio (1b), $W/2 \approx 6.077$ Mt.

The energy of a volcanic explosion can also be estimated by measuring the total electron content with GNSS [Heki, 2006]. Heki [2006] has proposed an empirical method that involves analyzing amplitudes of volcanic ionospheric disturbances relative to the background state of TEC and comparing the TEC response to explosions of known yield [Calais et al., 1998]. The explosion energy of the Asama volcano in Japan with $VEI$=2, estimated by this method, was $\sim 4 \cdot 10^4$ t in TNT equivalent or $2 \cdot 10^{14}$ J [Heki, 2006].

Note that along with the background electron content the amplitude of the volcanic ionospheric disturbances is additionally affected by two other factors — the magnetic field configuration and the angle between the line of sight of the source and the wavefront. Nonetheless, as Astafyeva et al. [2022] believe, in the case of the very strong eruption of the Hunga Tonga volcano the background TEC appeared to be significantly lower than the disturbed one, and the magnetic field configuration and the wavefront direction within geometric visibility at a rough estimate can be neglected. Thus, the explosive yield of the Hunga Tonga volcano eruption was estimated from 9 to 37 Mt in TNT equivalent [Astafyeva et al., 2022]. We can deduce that despite the difference in approaches to estimating the energy of the Hunga Tonga volcano eruption, the absolute value of the explosive yield is very large — tens of megatons in TNT equivalent.

## SUMMARY AND CONCLUSIONS

We have presented the results of the observation of acoustic waves from the major eruption of the Hunga Tonga volcano, which occurred in the southwestern Pacific Ocean on January 15, 2022. In this paper, primary analysis and interpretation of the results were carried out. We can draw the following conclusions.

The recorded acoustic signal has a complex structure similar to the wave structure of signals from powerful nuclear explosions, the Tunguska meteorite [Gossard, Hook, 1978], as well as to the acoustic signals from the Hunga Tonga volcano eruption presented in [Kulichkov et al., 2022; Dolgikh et al., 2022]. Such a waveform is interpreted as the result of a superposition of Lamb waves, infrasound, and IGW.

A characteristic time sequence three group of the arrivals in the head part of the signal (Lamb wave) has been revealed. This sequence is associated with three phases of the eruption: 1) strong explosion and destruction of Hunga Tonga island; 2) release of red-hot magma to the ocean surface and formation of a large amount of superheated steam pulsating in the atmosphere; 3) rise of a height eruptive column into the atmosphere, which can be a source of low-frequency acoustic radiation.

We have compared the acoustic signals from the Hunga Tonga volcano eruption recorded in Eastern Siberia and Alaska, and have estimated the mean signal propagation velocity along these paths. Recording the acoustic signal from the violent eruption of the Hunga Tonga volcano in various parts of Earth indicates the global nature of signal propagation.

Further work on this topic, in our opinion, requires combining the data obtained in Russia and concentrating efforts in developing a method for determining average characteristics of the atmosphere along the acoustic signal propagation path.

The data used in this work was obtained at the infrasound station included in ISTP SB RAS Shared Equipment Center “Angara” [http://ckp-rf.ru/ckp/3056]. The work was financially supported by Basic Project “Geophysical Monitoring and Complex Observations of Parameters of Earth’s Atmosphere and Near-Earth Space for Research in Solar-Terrestrial Physics” (No. 0278-2021-0004).

We are grateful to the reviewers who took the trouble to familiarize themselves with the work and made a number of comments that contributed to its significant improvement.

## REFERENCES

Adam D. Tonga volcano eruption created puzzling ripples in Earth’s atmosphere. *Nature*. 2022, vol. 601, p. 497. DOI: 10.1038/d41586-022-00127-1.

Adushkin V.V., Rybnov Yu.S, Spivak A.A. Geophysical effects of the eruption of Hunga-Tonga-Hunga-Haapai volcano on January 15, 2022. *Doklady Earth Sci.* 2022, vol. 504, no. 2, pp. 362–367. DOI: 10.1134/s1028334x22060034.

Astafyeva E., Maletckii B., Mikesell T.D., Munaibari E., Ravanelli M., et al. The 15 January 2022 Hunga Tonga eruption history as inferred from ionospheric observations. *Geo-*

*phys. Res. Lett*. 2022, vol. 49, e2022GL098827. DOI: 10.1029/2022GL098827.

Brachett N., Brown D., Mialle P., Le Bras R., Coyne J., Given J. Monitoring the Earth's Atmosphere with the Global IMS Infrasound Network. *Geophysical Research Abstracts.* 2010, vol. 12, EGU2010-10773.

Calais E., Minster J.B., Hofton M.A., Hedlin H. Ionospheric signature of surface mine blasts from Global Positioning System measurements. *Geophysical Journal International*. 1998, vol. 132, iss. 1, pp. 191–202. DOI: 10.1046/j.1365-246x.1998.00438.x.

Carpenter E.W., Harwood G., Whiteside T. Microbarograph records from Russian large nuclear explosions. *Nature*. 1961, Vol. 192, no. 4805, p. 847.

Dessler A.J. Infrasonic thunder. *J. Geophys. Res.* 1973, vol. 78, no. 12, pp. 1889–1896.

Dobrynin V.A., Sorokin A.G. Atmospheric effects of the volcano Tonga eruption. *Sbronik trudov XXXV sessii Rossiiskogo akusticheskogo obshchestva*. [Proc. the XXXV Session of the Russian Acoustic Society]. Moscow, GEOS Publ., 2023. DOI: 10.34756/GEOS.2023.17.38487. (In Russian).

Dolgikh G., Dolgikh S., Ovcharenko V. Initiation of infrasonic geosphere waves caused by explosive eruption of Hunga Tonga-Hunga Haapai volcano. *Journal of Marine Science and Engineering.* 2022, vol. 10, 1061. DOI: 10.3390/jmse10081061.

Donn W.L., Ewing M. Atmospheric waves from nuclear explosions. Part II. The Soviet Test 30 October, 1961. *J. Atmos. Sci*. 1962, vol. 19, iss. 3, pp. 264–273.

Duncombe J. The surprising reach of Tonga's giant atmospheric waves. *Eos*. 2022. DOI: 10.1029/2022EO220050.

Edwards W.N., Brown P.G., ReVelle D.O. Estimates of meteoroid kinetic energies from observations of infrasonic airwaves. *J. Atmos. Solar-Terr. Phys*. 2006, vol. 68, pp. 1136–1160. DOI: 10.1016/j.jastp.2006.02.010.

Fee D., Matoza R.S. An overview of volcano infrasound: From hawaiian to plinian, local to global. *J. Volcanology and Geothermal Res*. 2013, vol. 249, pp. 123–139. DOI: 10.1016/j.jvolgeores.2012.09.002.

Garrett C.J.R. Atmospheric edge waves. *Quart. J. Roy. Meteorological Soc*. 1969, vol. 95, pp. 731–753.

Garova E., Ferapontov I. Four signals of Hunga-Tonga Hunga-Haapai. The volcano explosion in the Pacific Ocean as looked from Moscow. *N Plus*. 21.01.2022. URL: https://nplus1.ru/material/2022/01/21/tonga (accessed June 12, 2023). (In Russian).

Gordeev E.I., Firstov P.P., Makhmudov E.R., Kulichkov S.N. Infrasonic waves from volcanic eruptions on the Kamchatka peninsula. *Izvestiya, Atmospheric and Oceanic Physics*. 2013, vol. 49, no. 4, pp. 420–431. DOI: 10.1134/S0001433813030080.

Gossard E., Hook U. Waves in the Atmosphere. Moscow, Mir, 1978, p. 532. (In Russian).

Gostintsev Ju.A., Ivanov E.A., Anisimov S.V., Pedanov M.V., Kulichkov S.N., Morduhovich M.I., et al. On the mechanism of generation of infrasound waves in the atmosphere by strong fires. *Doklady Akademii nauk* [Proceeding of Academy of Science USSR]. 1985, vol. 283, no. 3, pp. 573–576. (In Russian).

Harkrider D.C. Theoretical and observed acoustic-gravity waves from explosion sources in the atmosphere. *J. Geophys. Res*. 1964, vol. 69, no. 24, pp. 5295–5321.

Heki K. Explosion energy of the 2004 eruption of the Asama Volcano, central Japan, inferred from ionospheric disturbances. *Geophys. Res. Lett*. 2006, vol. 33, iss. 14, L14303. DOI: 10.1029/2006GL026249.

Kulichkov S.N. On the propagation of Lamb waves in the atmosphere over the surface. *Izvestiya AN SSSR. Fizika atmosfery i okeana* [Izvestiya of Academy of Science USSR. Atmospheric and Oceanic Physics]. 1987, vol. 23, no. 12. (In Russian).

Kulichkov S.N., Chunchuzov I.P., Popov O.E., Gorchakov G.I., Mishenin A.A, Perepelkin V.G., Bush G.A., et al. Acoustic-gravity Lamb waves from the eruption of the Hunga-Tonga-Hunga-Hapai volcano, its energy release and impact on aerosol concentrations and tsunami. *Pure and Applied Geophysics.* 2022, vol. 179, pp. 1533–1548. DOI: 10.1007/s00024-022-03046-4.

Maeda K., Young J.J. Propagation of the Pressure Waves Produced by Auroras. *Journal of Geomagnetism and Geoelectricity*. 1966, vol. 18, no. 2, pp. 275–299.

Martines-Bedenko V., Pilipenko V., Shiokawa K., Akbashev R. Electromagnetic ULF/ELF oscillations caused by the eruption of the Tonga volcano. *Solar-Terr. Phys*. 2023, vol. 9, iss. 1, pp. 47–55. DOI: 10.12737/stp-91202306.

Matoza R., Fee D., Assink J., Lezzi A., Green D., et al. Atmospheric waves and global seismoacoustic observations of the January 2022 Hunga eruption, Tonga. *Science*. 2022, vol. 377, iss. 6601, pp. 95–100. DOI: 10.1126/science.abo7063.

Pasko V.P. Mechanism of infrasonic pulses from thunderclouds. *J. Geophys. Res.* 2009, vol. 114, D08205. DOI: 10.1029/2008JD011145.

Pierce A.D., Pousey J.W. Theory of excitation and propagation of Lamb's atmospheric edge mode from nuclear explosions. *Geophys. J. Roy. Astron. Soc*. 1971, vol. 26, pp. 341–368.

ReVelle D.O. Historical detection of atmospheric impacts by large bolides using acoustic-gravity waves. *Annals of the New York Academy of Sciences*. 1997, vol. 822, pp. 284–302. DOI: 10.1111/j.1749-6632-1997.tb48347.xS.

Rybnov Yu.S., Soloviev S.P., Krasheninnikov A.V., Rybnov S.Yu. Geophysical fields variations during the eruption of the Hunga-Tonga-Hunga-Haapai volcano on January 15, 2022. *Dinamicheskie protsessy v geosferakh* [Dynamic Processes in Geospheres]. 2023, vol. 15, no. 1, pp. 63–72. DOI: 10.26006/29490995_2023_15_1_63. (In Russian).

Sorokin A.G. Infrasonic radiations Chelyabinsk meteoroid. *Solnechno-zemnaya fizika* [Solar-Terr. Phys.]. 2013, vol. 24, pp. 58–63. (In Russian).

Sorokin A.G., Dobrynin V.A. Method of studying infrasound waves from thunderstorms. *Solar-Terr. Phys*. 2022, vol. 8, iss. 1, pp. 62–68. DOI: 10.12737/stp-81202208.

Thurin J., Tape C., Modrak R. Multi-Event Explosive Seismic Source for the 2022 Mw 6.3 Hunga Tonga Submarine Volcanic Eruption. *The Seismic Records*. 2022, vol. 2, iss. 4, pp. 217–226. DOI: 10.1785/0320220027.

Vergoz J., Hupe P., Listowski C., Le Pichon A., Garcés M.A., Marchetti E., et al. IMS observations of infrasound and acoustic-gravity waves produced by the January 2022 volcanic eruption of Hunga Tonga: A global analysis. *Earth and Planetary Science*. 2022, vol. 591, 117639. DOI: 10.1016/j.epsl.2022.117639.

Wright C.J., Hindley N., Alexander M.J., Barlow M., Hoffmann L., Mitchell C., et al. Tonga eruption triggered waves propagating globally from surface to edge of space. *Earth and Space Science Open Archive*. 2022, vol. 609, iss. 7928, pp. 741–746. DOI: 10.1002/essoar.10510674.1.

Liu X., Xu J., Yue J., Kogure M. Strong gravity waves associated with Tonga volcano eruption revealed by SABER observations. *Geophys. Res. Lett*. 2022, vol. 49, iss. 10, e2022GL098339. DOI: 10.1029/2022GL098339.

Yamomoto R. The microbarographic oscillations produced by the explosions of hydrogen bombs. *Bull. Inst. Chem. Res. Kyoto Univ*. 1954, vol. 32, pp. 120–133.

Yerushchenkov A.I., Filippov A. Kh., Makukhin V.L. Infrasound waves from lightning discharge. *Issledovaniya po geomagnetizmu, aeronomii i fizike Solntsa* [Res. on Geomagnetism, Aeronomy and Solar Physics]. 1976, iss. 38, pp. 73–78. (In Russian).

URL: https://twitter.com/NWSAlaska/status/1482431322740060162?cxt=HHwWhMCrveHb05IpAAAA (accessed June 12, 2023; 2023).

URL: https://www.reuters.com/graphics/TONGA-VOLCANO/LIGHTNING/zgpomjdbypd/ (accessed June 12, 2023).

Original Russian version: Sorokin A.G., Dobrynin V.A., published in Solnechno-zemnaya fizika. 2024. Vol. 10. Iss. 1. P. 59–67. DOI: 10.12737/szf-101202408. 

*How to cite this article*

Sorokin A.G., Dobrynin V.A. Registration of the atmospheric effect of the Hunga Tonga volcano eruption. *Solar-Terrestrial Physics*. 2024. Vol. 10. Iss. 1. P. 54–62. DOI: 10.12737/stp-101202408.